Biochemistry and Biophysics Reports 7 (2016) 230–239

Contents lists available at ScienceDirect

Biochemistry and Biophysics Reports

journal homepage: www.elsevier.com/locate/bbrep

SOX2 suppresses the mobility of urothelial carcinoma by promoting the expression of S100A14

Moon-Sing Lee [a,b,1], Wan-Ting Hsu [c,1], Yi-Fang Deng [c], Ching-Wei Lin [c], Erh-Ying Weng [c], Hsin-Ping Chang [c], Shu-Fen Wu [c], Chin Li [c,*]

[a] Department of Radiation Oncology, Buddhist Dalin Tzu Chi Hospital, Chiayi, Taiwan
[b] School of Medicine, Tzu Chi University, Hualien, Taiwan
[c] Department of Life Science, National Chung Cheng University, Chiayi, Taiwan

ARTICLE INFO

Article history:
Received 2 February 2016
Received in revised form
27 May 2016
Accepted 21 June 2016
Available online 25 June 2016

Keywords:
SOX2
S100A14
RNA binding protein
Post-transcriptional regulation

ABSTRACT

Sex-determining region Y (SRY)-box protein 2 (SOX2) plays a critical role in stem cell maintenance and carcinogenesis. In addition to its function as a minor-groove DNA binding transcription factor, our previous study showed that SOX2 also acts as a RNA binding protein. In current study, we first showed that SOX2 displayed high affinity toward the mRNA encoding S100A14 in BFTC905 and that depletion of SOX2 resulted in a decrease of S100A14 mRNA and protein level. To characterize the RNA binding sequence recognized by SOX2, oligomer-directed RNase H digestion was coupled to the cross-linking before immunoprecipitation assay to demonstrate that SOX2 preferentially binds to the 3′-UTR of the S100A14 mRNA. Using EGFP-S100A14 3′-UTR reporters and mobility shift assay, we identified that the binding sequence on the 3′-UTR of the S100A14 mRNA exhibits a stem-loop structure. Together, our data indicates that SOX2 enhances S100A14 expression by binding to the 3′-UTR of the S100A14 mRNA. Functionally, depletion of SOX2 increases growth and mobility of BFTC905. Knock-down of S100A14 in BFTC905 also leads to an increase in the number of the cells in the S phase and higher mobility, suggesting that SOX2 suppresses cell growth and mobility through promoting the expression of S100A14. Together, our experimental evidence indicates that SOX2 is capable of exerting its cellular functions by functioning as an RNA binding protein in post-transcriptional regulation.

1. Introduction

Post-transcriptional regulation mechanisms, including alternative splicing, mRNA stability, and translation modulation, play a major role in creating transcriptome and proteome complexity. Mechanistically, it is essential to select correct RNA transcripts for regulation [1,2]. The trans-acting guide-RNA-carrying protein complexes and RNA binding proteins are responsible to achieve the target specificity by recognizing the cis-sequence elements on the RNA transcripts. While the guide RNA-protein complexes, which are typified by microRNA-loaded RNA-induced silencing complex (RISC), achieve sequence-specific recognition through complementary annealing of the guide RNA [3], RNA binding proteins bind to the target RNA sequences through the RNA binding domains [4]. It was estimated that the human genome encodes hundreds of RNA binding proteins, but only limited numbers of the RNA binding protein repertoire have been extensively studied [5–7]. Given the important role of post-transcriptional regulation in cellular functions, it is necessary to advance our understanding on the functions of RNA binding proteins.

RNA binding proteins binds to the target RNA transcripts through sequence-specific RNA-binding domains [8]. Although most of RNA binding proteins possess RNA-specific interaction domains, such as the RNA recognition motif (RRM) and hnRNP K homologous domain (KH domain) [8–10], some DNA binding proteins were shown to exhibit RNA binding capabilities. One of such versatile nucleic acid binding motifs is the zinc-finger DNA-binding domain [11,12]. The most notable example dual function transcription factor is Wilm's tumor 1 (WT1), the master regulator for the development of the urinary and reproductive systems in mammals [13–15]. WT1 interacts with splicing factor and RNA binding protein, including U2AF65, WTAP, and RBM4. As the result of its RNA binding activity, WT1 performs diverse post-transcriptional activities, including 3′ splice site selection in the nucleus as well as mRNP localization and translation regulation in the cytoplasm [16–18]. Recently, p53, which is also a zinc-finger protein, was implicated in microRNA biogenesis by facilitating the

* Corresponding author.
E-mail address: biocl@ccu.edu.tw (C. Li).
[1] These authors contributed equally to this work.

http://dx.doi.org/10.1016/j.bbrep.2016.06.016

recognition of the stem-loop structure on the primary microRNA [19], further supporting the zinc-finger domain can be used as DNA binding as well as post-transcriptional RNA recognition.

Another group of the dual function transcription factors is the members of the SOX family. The conserved nucleic acid recognition domain of the SOX proteins is the high-mobility group (HMG) box domain [20,21]. Among the SOX proteins, SRY, SOX6, and SOX9 were shown to facilitate pre-mRNA splicing in HeLa nuclear extracts *in vitro* [22]. In addition, the RNA-binding domain of human hepatitis D virus exhibits a structure similar to that of the SRY HMG box [23]. Although these findings indicate that the HMG domain is also used for the recognition of the RNA sequences, the cellular functions of the SOX family of proteins in post-transcriptional gene regulation have not been extensively studied.

SOX2 plays an essential role in stem cell maintenance program. Because SOX2 exhibits DNA binding activity and acts cooperatively with Oct4 in the stem cell maintenance pathway [24,25], it is often assumed that SOX2 exerts its function by regulating transcription. We previously reported that SOX2 is expressed in BFTC905 cells, an urothelial carcinoma cell line retaining partial epithelial characteristics [26]. Our data also showed that the expression of SOX2 leads to alternative splicing of the adenovirus early gene 1 A (E1A). Recombinant SOX2 also directly binds to the E1A pre-mRNA *in vitro*, indicating that SOX2 exhibits RNA-binding activity. Here, we report that SOX2 binds to the 3′-UTR of the S100A14 mRNA and promotes its expression. Depletion of either SOX2 or S100A14 reduced the growth and mobility of BFTC905 cells, suggesting that SOX2 exerts its cellular function through post-transcriptionally regulating the expression of S100A14. Thus, our study provides experimental evidence to support the notion that the SOX proteins are dual function proteins, acting as both transcription factors and RNA binding proteins.

2. Materials and methods

2.1. Plasmids and cell culture

BFTC905 was cultured in RPMI 1640 medium supplemented with 1.5 g/L sodium bicarbonate and 15% fetal bovine serum (Sigma-Aldrich, St. Louis, MO, USA), and HEK293T was cultured in DMEM medium supplemented with 10% fetal bovine serum. Knock-down of targeted genes was achieved by employing the short-hairpin RNA (shRNA)-expressing lentiviral vectors obtained from the National RNAi Core Facility (Academia Sinica, Taipei, Taiwan). The identification number of the anti-SOX2 shRNA clone used in transcriptome analysis and subsequent cellular function experiment is TRCN00000355638 with the targeted sequence 5′-CCCTGCAGTACAACTCCATGA. An additional anti-SOX2 shRNA clone, TRCN00000231641, was used to generate second cell line, designated as BFTC905/shSOX2-41. The targeted sequences of this anti-SOX2 shRNA is 5′-CAACGGCAGCTACAGCATGAT. The identification number of the anti-S100A14 shRNA clone is TRCN0000056527, and the targeted sequence is 5′-CCTCATCAAGAACTTTCACCA. pLKO.1-shLuc, the vector expressing the anti-luciferase shRNA, served as a control. To generate the viral particles for infection, the shRNA-expressing vectors were co-transfected with pCMV-ΔR8.91 and pMD. G into HEK293T using Turbofect transfection reagent (Thermo Fisher Scientific, Waltham, MA). The packaged viruses were harvested from the culture medium and used to infect BFTC905. Forty-eight hours after infection, BFTC905 was selected against puromycin to obtain the stable shRNA-expressing cell lines BFTC905/shLuc, BFTC905/shSOX2, BFTC905-shSOX2–41, and BFTC905/shS100A14. BFTC905/shLuc and BFTC905/shSOX2 were subsequently transfected with pTagRFP-N (Evrogen, Moscow, Russia) and pEGFP-C1 (Takara, Kyoto, Japan), respectively. The fluorescent protein-positive cells were selected against 400 μg/ml G418 for two weeks and isolated using a FACS Aria cell sorter (BD Biosciences, San Jose, CA, USA) to obtain the BFTC905/shLuc-RFP and BFTC905/shSOX2-EGFP cells. SOX2 was also cloned from pcDNA-SOX2 into pTagRFP-N to create pSOX2-RFP. The pEGFP-hnRNP A1 and pEGFP-hnRNP C1 plasmids were obtained from Dr. W. Y. Tarn (Institute of Biomedical Science, Academia Sinica).

To create the S100A14 3′-UTR reporters, we first obtained the fragmented sequence of the S100A14 3′-UTR from the BFTC905 cells by reverse transcription-PCR and subsequently cloned these fragments into pEGFP-C1 to create the EGFP-S100A14 3′-UTR fragment reporters. These fragments correspond to the S100A14 mRNA sequence at nt 471-589, 566-622, 643-784, 758-866, 842-930, and 907-1018. A translation stop codon was incorporated into the 5′-end of the amplified sequences to prevent these sequences from being translated. These reporters were transfected into BFTC905 with either pcDNA5/TO-β-galactosidase or pcDNA5/TO-FLAG-SOX2. The transfected cells were selected against 50 μg/ml hygromycin for 48 h before harvest.

2.2. Cell growth determination and cell cycle analysis

To determine the growth rate, 1, 0.5, 0.25, 0.125 million BFTC905/shLuc and BFTC905/shSOX2 cells were seeded in plates and cultured for one, two, three, or four days, respectively. At the end of the time period, the cells were washed with PBS, fixed in 4% paraformaldehyde, and stained with 0.01% crystal violet in water for 30 min. The cells were then washed four times with water, dried, and extracted with 20% acetic acid. The absorbance of the acid extracts was measured at 595 nm. For the cell cycle analysis, the cells were harvested and fixed in 100% ethanol at −20 °C for at least 24 h. The fixed cells were treated with 5 mg/ml RNase A and 40 μg/ml propidium iodide at 37 °C for 30 min, followed by analysis by flow cytometry.

2.3. Wound healing and transwell migration assays

In each chamber of the culture inserts, 20,000 control or SOX2 knocked-down cells were seeded and cultured in the medium with 2% serum for 16 h. The inserts were then removed, and images were taken at 0, 12, and 24 h. The transwell assay was performed by seeding 10,000 fluorescent protein-tagged cells in the upper chamber in normal culture medium for 24 h. The medium in the upper chamber was then replaced with the medium containing 1% serum. After additional 24 h incubation, the cells were fixed in 4% paraformaldehyde for 10 min. After fixation, the total cell population was imaged using a fluorescence microscope with a CCD camera. The cells on the upper chamber were then removed, and the cells in the lower chamber were imaged using an Olympus FV1000 laser scanning microscope.

2.4. Immunoblotting

Immunoblotting was performed as described below. The protein samples were first separated by SDS-polyacrylamide gel electrophoresis and transferred to a Hybond-P membrane (GE Healthcare Life Sciences, Waukesha, WI, USA). The protein-bound membrane was blocked in 5% skim milk in phosphate-buffered saline (PBS) containing 0.1% Tween 20, followed by hybridization of the primary antibodies overnight at 4 °C. The secondary antibodies used for detection were horseradish peroxidase-conjugated anti-mouse and anti-rabbit goat polyclonal antibodies (Sigma-Aldrich). After hybridization of the secondary antibodies and extensive washing, chemiluminescence detection was performed using the Immobilon Western Chemiluminescent HRP Substrate

(EMD Millipore, Billerica, MA, USA). The primary antibodies used for immunoblotting were anti-SOX2 (Abcam, Cambridge, UK), anti-S100A14 (Proteintech, Chicago, IL, USA) and anti-α-tubulin (Thermo Fisher) antibodies.

2.5. Reverse transcription-polymerase chain reaction (RT-PCR) and quantitative RT-PCR (qRT-PCR)

The oligomers used in this study are listed in the supplemental material (Table S1). Total RNA was purified from the cultured cells using TRIZOL reagent (Thermo Fisher) according to the manufacturer's protocol. The cDNAs were subsequently prepared from the total RNA using MMLV high-performance reverse transcriptase (Illumina, San Diego, CA, USA) and oligo(dT) as the primer. The condition for PCR detection was 32 cycles of amplification of the template by denaturing at 94 °C for one minute, primer annealing at 55 °C for 30 s, and product extension at 72 °C for 1 min. Quantitative RT-PCR was performed using GoTag qPCR master mix (Promega, Madison, WI, USA) in a StepOne real-time PCR system (Thermo Fisher). The condition for 40 cycles of amplification was template denaturing at 94 °C for one minute, primer annealing at 55 °C for 30 s, and product extension at 72 °C for 45 s.

2.6. In vitro RNA pull-down assay

To identify the cellular mRNA target of SOX2, total RNA purified from the BFTC905 cells was used in the *in vitro* pull-down assay. The unbound RNA was purified from the supernatant using TRIZOL reagent (Thermo Fisher). Precipitated RNA was released from the matrix by proteinase K digestion and purified using TRIZOL reagent, with glycogen as the precipitation carrier. Purified RNA samples were amplified using the MessageAmp aRNA kit (Thermo Fisher) and analyzed using a whole genome DNA microarray (Human OneArray, Phalanx Biotech Group, HsinChu, Taiwan). The data were submitted to Gene Expression Omnibus, NCBI, USA (accession number GSE33207).

2.7. Massive parallel sequencing

Massive parallel sequencing was analyzed on the Illumina platform. Total RNA was extracted from the BFTC905/shLuc and BFTC905/shSOX2 cells. The integrity of purified RNA was evaluated by capillary electrophoresis in a 2100 Bioanalyzer (Agilent, Santa Clara, CA, USA). The library was prepared with the TrueSeq Stranded RNA Sample Prep Kit (Illumina). Sequencing was performed on an Illumina Miseq sequencer and provided 10,268,595 and 11,419,579 paired-end 150-base reads for BFTC905/shLuc and BFTC905/shSOX2, respectively. The sequences were mapped to the human genome hg19 using TopHat 2. Annotation and estimation of gene expression (reads per kilobase per million [RPKM]) was performed using Cufflink and Cuffcompare. The data were submitted to Gene Expression Omnibus, NCBI, USA (accession number GSE54136).

2.8. Cross-linking before immunoprecipitation (CLIP) assay and oligomer-dependent RNase H digestion

The CLIP assay was performed as following. The BFTC905 cells were washed twice with PBS and irradiated with 50 mJ/cm^2 of 365 nm UV light. The cells were then lysed in radioimmunoprecipitation assay buffer (RIPA) containing 10 mM sodium phosphate (pH 7.2), 150 mM sodium chloride, 2 mM EDTA, and 1% NP-40 on ice in the presence of RNase inhibitors (Thermo Fisher). The lysate was then subjected to DNase I (Promega) digestion at 37 °C for 30 min. After removing the undissolved debris by centrifugation at 4 °C and 14,000 g for 30 min, the supernatant was subjected to immunoprecipitation using antibody-coated protein A agarose beads (Sigma-Aldrich) at 4 °C for 2 h. The antibodies used in CLIP assay were non-immunized control antibodies (Santa Cruz Biotechnology, Santa Cruz, CA), anti-SOX2 antibody (Cell Signaling, Danvers, MA), and anti-FLAG M2 antibody (Sigma). The beads were washed extensively three times with RIPA buffer containing 0.1% NP-40. The RNAs associated with the matrix and in the supernatant were then digested with proteinase K at 37 °C for 30 min, followed by purification using TRIZOL reagent. The cDNAs were prepared as described above, and the presence of the target mRNAs was detected by RT-PCR. To digest the S100A14 mRNA at specific locations, we performed oligomer-dependent RNase H digestion on the matrix-bound mRNA after immunoprecipitation. The CLIP procedure was followed until the precipitation step was completed. Then, the beads were washed and incubated in the RIPA buffer containing the targeting oligomer and 20 units of RNase H (Illumina) at 37 °C for one hour. The RNAs in the supernatant and on the beads were recovered and analyzed by RT-PCR.

2.9. Electrophoretic mobility shift assay (EMSA)

The T7-3′-UTR fragment constructs were prepared by annealing the T7 forward oligomer with the antisense T7-3′-UTR oligomers, followed by purification through MicroSpin G-25 columns (GE Healthcare Life Sciences). The RNA oligomers were produced by *in vitro* transcription using T7 RNA polymerase (Promega) in the presence of [P32]-α-UTP and purified by ethanol precipitation. For each reaction, 2500 cpm of the radiolabeled RNA oligomer in 2 μl of RIPA buffer with 1 mM $MgCl_2$ was mixed with 2 μl of the cell extract and incubated at room temperature for 20 min. After incubation, 2 μl of loading dye was added to the reaction, and the reaction mix was analyzed on a 4% non-denaturing polyacrylamide gel with 5% glycerol at 4 °C. After electrophoresis, the gel was dried and the image was obtained by autoradiography.

2.10. Heterokaryon assay

The pSOX2-RFP plasmid was co-transfected into HeLa cells with pEGFP-hnRNP A1 or pEGFP-hnRNP C1 for 24 h. NIH 3T3 cells were seeded to the culture and allowed to adhere for 2 h. Co-cultured cells were treated with 50 μg/ml cyclohexamide for 2.5 h and then 100 μg/ml cyclohexamide for 0.5 h. The cells were fused by treating the cultures with 50% polyethylene glycol 3350 for 90 s, followed by extensive washing with PBS and continued culture for 4 h. The cells were also fixed in 4% paraformaldehyde and counterstained with Hoechst 33250. The fluorescent images were captured using an Olympus FV1000 laser scanning microscope.

3. Results

3.1. SOX2 binds to the S100A14 mRNA and regulates its cellular level

We previously identified the RNA binding activity of SOX2. The result suggests that SOX2 potentially participates in post-transcriptional regulation as an RNA binding protein. In this study, we first set out to identify the mRNAs directly bound by SOX2. To screen for SOX2 binding targets, an *in vitro* pull down assay was performed using control GST or GST-SOX2 fusion protein to precipitate total RNA purified from the BFTC905 cells. The RNA samples were prepared from the supernatant and matrix-bound fractions and subsequently analyzed by expression microarray. However, the amount of RNA precipitated by GST was nearly undetectable and insufficient for analysis. Thus, we compared the mRNA profiles from the supernatant and precipitation fractions of the SOX2 pull down reaction to the profile from the supernatant

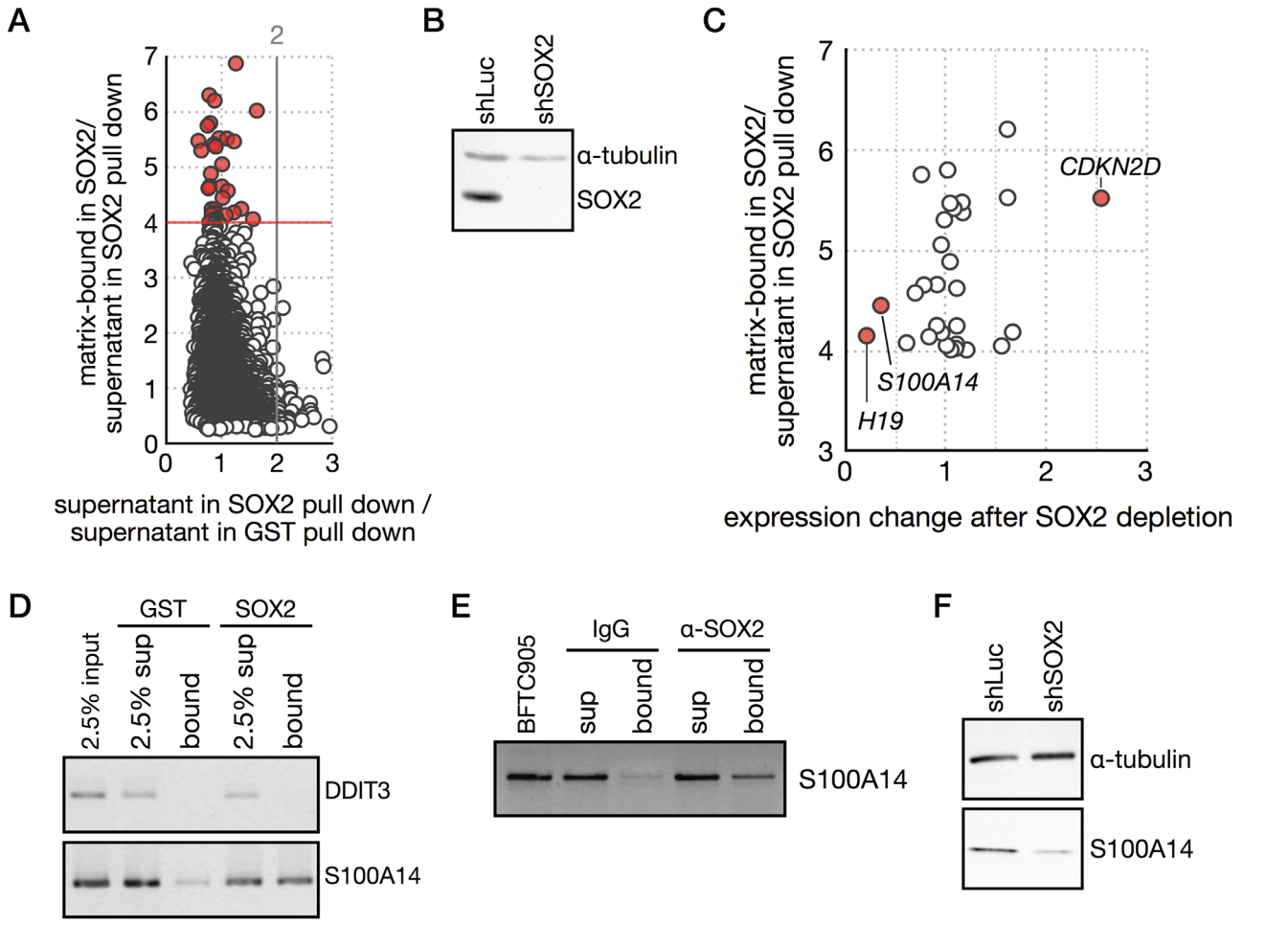

Fig. 1. SOX2 binds to and regulates the expression of the S100A14 mRNA in BFTC905. (A) Recombinant SOX2 was used as a bait protein to precipitate purified the total RNA from the BFTC905 cells in *in vitro* pull-down assays. GST served as the negative control. The RNA was purified from supernatant and precipitated fractions, followed by microarray analysis. The genes preferentially bound by SOX2 were indicated in red. (B) BFTC905/shLuc and BFTC905/shSOX2 cells were created by infecting the BFTC905 cells with shRNA-expressing lentiviral vectors. Suppression of SOX2 was confirmed by immunoblotting. (C) Massive parallel sequencing was performed to analyze the transcriptome of the BFTC905/shLuc and BFTC905/shSOX2 cells. The genes indicated in (A) was plotted against the expression change. Red color indicates more than 2-fold change in BFTC905/shSOX2. (D) The *in vitro* pull-down assay was performed using GST and SOX2 as the bait proteins. The level of the S100A14 mRNA in the input, supernatant, and precipitated fractions was determined by RT-PCR. DDIT3 serves as the non-enrichment negative control. (E) The CLIP assay was performed using either control IgG or anti-SOX2 antibodies. The RNA was recovered from the supernatant and the matrix, and the presence of the S100A14 transcript was detected by RT-PCR. and (F) The level of the S100A14 protein in the BFTC905/shLuc and BFTC905/shSOX2 cells was determined by immunoblotting. α-tubulin serves as the control.

fraction of the control reaction. While only 68 genes showed more than 2-fold change between the supernatant fractions of the control and SOX2 pull-down reactions, the SOX2-precipitated fraction had 733 and 1011 genes with more than 2-fold decrease and increase than the control, respectively. This drastic difference in profile indicated that SOX2 displayed binding specificity for a subset of cellular mRNA. The precipitation efficiency was then represented by the ratio between the supernatant and precipitation fractions of the SOX2 pull down reaction (Fig. 1A). Among the genes enriched in the SOX2 precipitation fraction, 124 genes showed more than 3-fold increase and were selected for further investigation (Fig. 1A).

Post-transcriptional regulation controls gene expression by modulating mRNA stability and translation efficiency. In this study, we focused on the genes with mRNA level post-transcriptionally regulated by SOX2. To achieve this goal, we suppressed the expression of SOX2 in BFTC905 (Fig. 1B) and determined the change in gene expression profile by massive parallel sequencing. To avoid false identification of candidate genes, an FPKM of 2 was arbitrarily used as a threshold to select genes of sufficient reads for further analysis. In the 10,381 genes with an FPKM larger than 2, approximately 3% of the genes showed more than 2-fold change in SOX2-depleted BFTC905. Cross-referencing the results of the *in vitro* RNA pull-down assay and expression profile analysis indicated that S100A14, CDKN2D, and H19 were enriched in SOX2 precipitation fraction and simultaneously showed significant change upon depletion of SOX2 in BFTC905 (Fig. 1C). S100A14 has been implicated in oncogenesis [27,28], but the mechanism by which it is regulated in SOX2-positive urothelial carcinoma has not been investigated. Hence, we focused our subsequent investigation using S100A14 as a model to illustrate the post-transcriptional function of SOX2. Direct interaction of SOX2 with the S100A14 mRNA was validated by detecting the presence of the S100A14 mRNA in the precipitation fraction (Fig. 1D). The CLIP assay also clearly showed that the S100A14 mRNA was preferentially enriched in the SOX2-precipitated fraction (Fig. 1E). Moreover, depletion of SOX2 also led to a decrease in the protein level of S100A14 (Fig. 1F), an observation also made in second SOX2-depleted BFTC905 line (Fig. S2B). In TSGH8301, an urothelial carcinoma cell line with extremely low SOX2expression, ectopic expression of SOX2 greatly increased the expression of S100A14 (Fig. S3A). Together, our data indicated a regulation circuit that SOX2 promotes S100A14 expression by binding to and stabilizing its transcript.

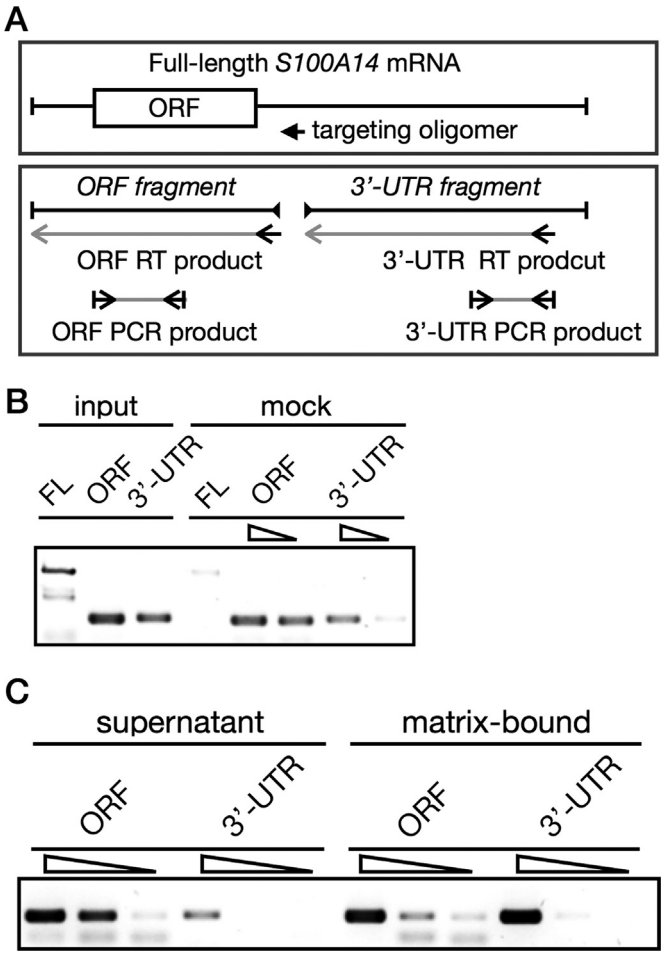

Fig. 2. SOX2 interacts with the 3′-UTR of the S100A14 mRNA *in vivo*. (A) The diagram depicts the annealing positions of the targeting oligomer for RNase H digestion and the primers for reverse transcription and PCR detection of the ORF and 3′-UTR fragments. (B) FLAG-SOX2 was transiently expressed in BFTC905 cells for 48 h, followed by the CLIP assay. The matrix-bound mRNA was incubated at 37 °C with RNase H in the absence of the targeting oligomer for 30 min. The mock-treated matrix-bound mRNA was then purified and reverse-transcribed. The full-length, ORF, and 3′ fragments of the S100A14 mRNA were detected by RT-PCR. (C) After immunoprecipitation, the matrix-bound mRNA was subject to oligomer-dependent RNase H digestion at 37 °C for 30 min. The ORF and 3′-UTR fragments of the S100A14 mRNA in the supernatant and bound to the matrix were recovered, reverse transcribed, and detected by semi-quantitative PCR.

3.2. SOX2 binds directly to a hairpin structure in the 3′-UTR of the S100A14 mRNA

Post-transcriptional regulation depends on the recognition of the 3′-UTR sequences by trans-acting regulatory factors [29,30]. It is likely that SOX2 regulates S100A14 through a similar mechanism. To determine whether SOX2 binds to the S100A14 3′-UTR, we coupled the CLIP assay with oligomer-dependent RNase H digestion. The target sequence of the antisense oligomer is located at the 5′-end of the S100A14 3′-UTR. Cleavage of the S100A14 mRNA by RNase H produces the ORF and 3′-UTR fragments, and the ORF and 3′-UTR fragments was detected by RT-PCR (Fig. 2A). Transiently expressed FLAG-SOX2 was immunoprecipitated from BFTC905, and RNase H digestion was performed in the absence (Fig. 2 B) or presence (Fig. 2C) of the targeting antisense oligomer. In the absence of the targeting oligomer, detection of the full-length product indicated that the RNase H treatment alone does not compromise the integrity of the S100A14 mRNA on the matrix (Fig. 2B). In contrast, most of the ORF fragment was released from the matrix to the supernatant after digestion in the presence of the antisense oligomer, while the majority of the 3′-UTR fragment was still bound to the matrix (Fig. 2C). Hence, the result clearly showed that SOX2 preferentially binds to the 3′-UTR of S100A14.

The length of the S100A14 3′-UTR is approximately 650 nucleotides. To locate the SOX2 binding site in the 3′-UTR, we dissected the 3′-UTR into 6 fragments and cloned the 3′-UTR fragments to the pEGFP-C2 vector. An in-frame stop codon was placed between the EGFP ORF and the cloned fragments, making the cloned fragments functioning as the 3′-UTR of the EGFP reporter mRNA. The structures of the S100A14 3′-UTR reporters are depicted in Fig. 3A. The reporters were expressed with FLAG-tagged SOX2 in BFTC905, and the interaction between SOX2 and the 3′-UTR reporter mRNA was examined by the CLIP assay. The result showed that the S100A14 643-784 sequence was precipitated by SOX2 with approximately 25-fold higher efficiency than that of the control EGFP mRNA (Fig. 3B and C), indicating that this region contains the SOX2 binding site.

We next dissected the 3′-UTR sequence between nucleotide 643 and 784 into six 32-nucleotide-long fragments with a 10 nucleotide overlap between them (Fig. 3D). These sequences were then used to generate radiolabeled RNA oligomers *in vitro*. These probes were incubated with the extracts prepared from BFTC905 with transiently expressed SOX2 or control β-galactosidase, and the protein-RNA mix was analyzed by non-denaturing acrylamide gel electrophoresis. Among these probes, the probes 687-718 and 709-740 showed retarded mobility. Furthermore, ectopic expression of SOX2 increases the retardation of probe 684-710, but not probe 710-740 (Fig. 3E), indicating that the sequence element for SOX2 binding resides in the sequence between nucleotide 684 and 710. A structural analysis of the sequence revealed that this sequence forms an stem-loop structure (Fig. 3F). Thus, our data demonstrated that SOX2 binds to a stem-loop structure in the 3′-UTR of the S100A14 mRNA.

3.3. SOX2 shuttles between the nucleus and cytoplasm

Many trans-acting RNA binding proteins are predominantly localized in the nucleus where initial binding to the target mRNA occurs. The protein-mRNA complexes are exported to the cytoplasm for execution of the regulatory pathway, and these RNA binding proteins then shuttle back to the nucleus after releasing from the complex [31]. Lacking a nuclear export signal, SOX2 can not be exported back to the cytoplasm in a CRM1-dependent pathway. Thus, the shuttling activity of SOX2 would be due to through the formation and export of the mRNA-protein complex. To demonstrate the shuttling activity of SOX2, we performed the heterokaryon assay to examine whether SOX2 will return to the cytoplasm from the nucleus. For this assay, SOX2-RFP was co-expressed with either EGFP-hnRNP A1 or EGFP-hnRNP C1 in HeLa cells, followed by fusion with NIH3T3 cells. As shown in Fig. 4, the result of the heterokaryon assay indicates that SOX2-RFP exhibited similar intracellular movement as EGFP-hnRNP A1 (Fig. 4, panels A–F). Meanwhile, EGFP-hnRNP C1 remained restricted to the nuclei (Fig. 4, panels G–L). Although the shuttling movement of SOX2-RFP appears to be slower than hnRNP A1-EGFP, our data still added support to the notion that SOX2 binds to the target mRNA in the nucleus and is subsequently transported to the cytoplasm as a component of the mRNP.

3.4. Suppression of SOX2 promotes the growth and mobility of BFTC905 cells

We next examined the cellular function of SOX2 in BFTC905. Compared to the control BFTC905/shLuc, BFTC905/shSOX2 displayed a slightly faster growth rate (Fig. 5A). Cell cycle analysis showed that the percentage of BFTC905/shSOX2 cells in S and G1

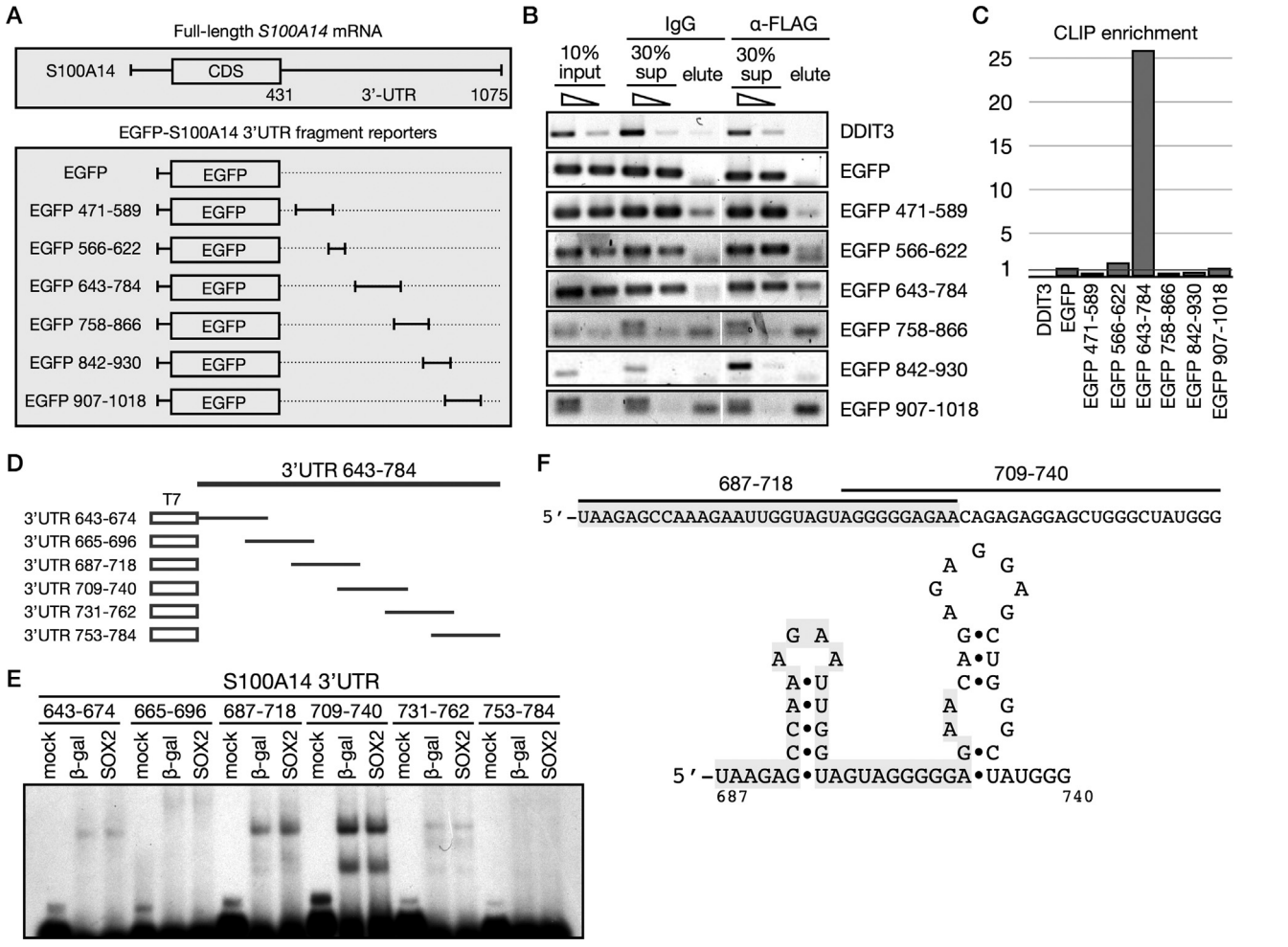

Fig. 3. The SOX2 binding site displays extensive secondary structure. (A) The diagram depicts the structures of the EGFP-S100A14 3′-UTR fragment reporters. Each 3′-UTR fragment was cloned into pEGFP-C2 with an in-frame translation stop codon located at the 5′-end of the fragment. (B) The EGFP-S100A14 3′-UTR reporters were co-expressed with FLAG-SOX2 in BFTC905 cells for 72 h. The CLIP assay was performed using the control IgG and anti-SOX2 antibodies. The EGFP-3′-UTR fragment mRNAs in the input, supernatant, and bound to the matrix were detected by RT-PCR to amplify the EGFP coding sequence. DITT3 serves as negative control. (C) The band intensities in (B) were quantified using ImageJ. The enrichment of the S100A14 3′-UTR reporters were calculated by following formula: [FLAG elute/(FLAG sup+FLAG sup)]/[IgG elute/(IgG sup+IgG elute)]. (D) The diagram depicts the sequences of the oligomers used to produce the 32-mer EGFP-S100A14 3′-UTR RNA fragments. (E) The *in vitro* synthesized RNA was incubated with β-galactosidase or SOX2-expressing BFTC905 cell extracts and analyzed by non-denaturing polyacrylamide electrophoresis. (F) The primary sequence between nt 687 and 740 was listed. The RNA oligomer for nt 687-718 is the sequence in gray box. The secondary structure of the S100A14 sequence between nt 687 and 740 predicted by Mfold is shown.

phases was slightly increased and decreased, respectively (Fig. S1). Together, the result suggests that suppression of SOX2 endows BFTC905 a slight growth advantage. Our unpublished data showed that the percentage of the SOX2-positive cells is often limited in the clinical specimens, indicating a mixed tumor cell population in the tumor mass (data not shown). Thus, we further tagged the control BFTC905/shLuc and SOX2-depleted BFTC905/shSOX2 cell lines with the TagRFP and EGFP fluorescence proteins. These two cell lines, BFTC905/shLuc-TagRFP and BFTC905/shSOX2-EGFP, were then mixed together and co-cultured for 15 days to simulate the coexistent environment in the tumor mass. At days 0 and 15, the percentage of BFTC905/shSOX2-EGFP cells in the population was determined by randomly imaging the cell population using a confocal laser scanning microscope (Fig. 5B). At the end of the 15-day period, the percentage of BFTC905/shSOX2-EGFP cells in the population was approximately more than 50% even though the initial percentage was relatively low (Fig. 5C), We also examined the growth of an additional BFTC905/shSOX2 cell line and found that it also displayed an increase in growth (Fig. S2C), further supporting our finding. Together, our data indicate that expression of SOX2 slows the growth of BFTC905.

In addition to the growth rate, we examined whether depletion of SOX2 alters the mobility of BFTC905. In the wound healing assay, the BFTC905/shSOX2 cells narrowed the gap more rapidly than the control BFTC905/shLuc cells (Fig. 5D), a finding collaborated by second SOX2-depleted BFTC905 (Fig. S2D). In contrast, expression of SOX2 decreased the mobility of S100A14 (Fig. S3B). We also examined the effect of SOX2 suppression by seeding mixed BFTC905/shLuc-TagRFP and BFTC905/shSOX2-EGFP cells in the upper chamber of the transwell apparatus. Twenty-four hours after removing the serum from the upper chamber, those cells that had migrated to the lower chamber were identified by fluorescence imaging. The result showed that there were significantly more BFTC905/shSOX2-EGFP cells migrating to the lower chamber, demonstrating an increase of mobility upon depletion of SOX2 (Fig. 5E). Thus, our data suggests that SOX2 likely act as a tumor suppressor in BFTC905.

3.5. Suppression of S100A14 leads to an increase in the growth and mobility of BFTC905 cells

Our data has established that SOX2 binds to the 3′-UTR of the S100A14 mRNA and that depletion of SOX2 resulted in a decrease

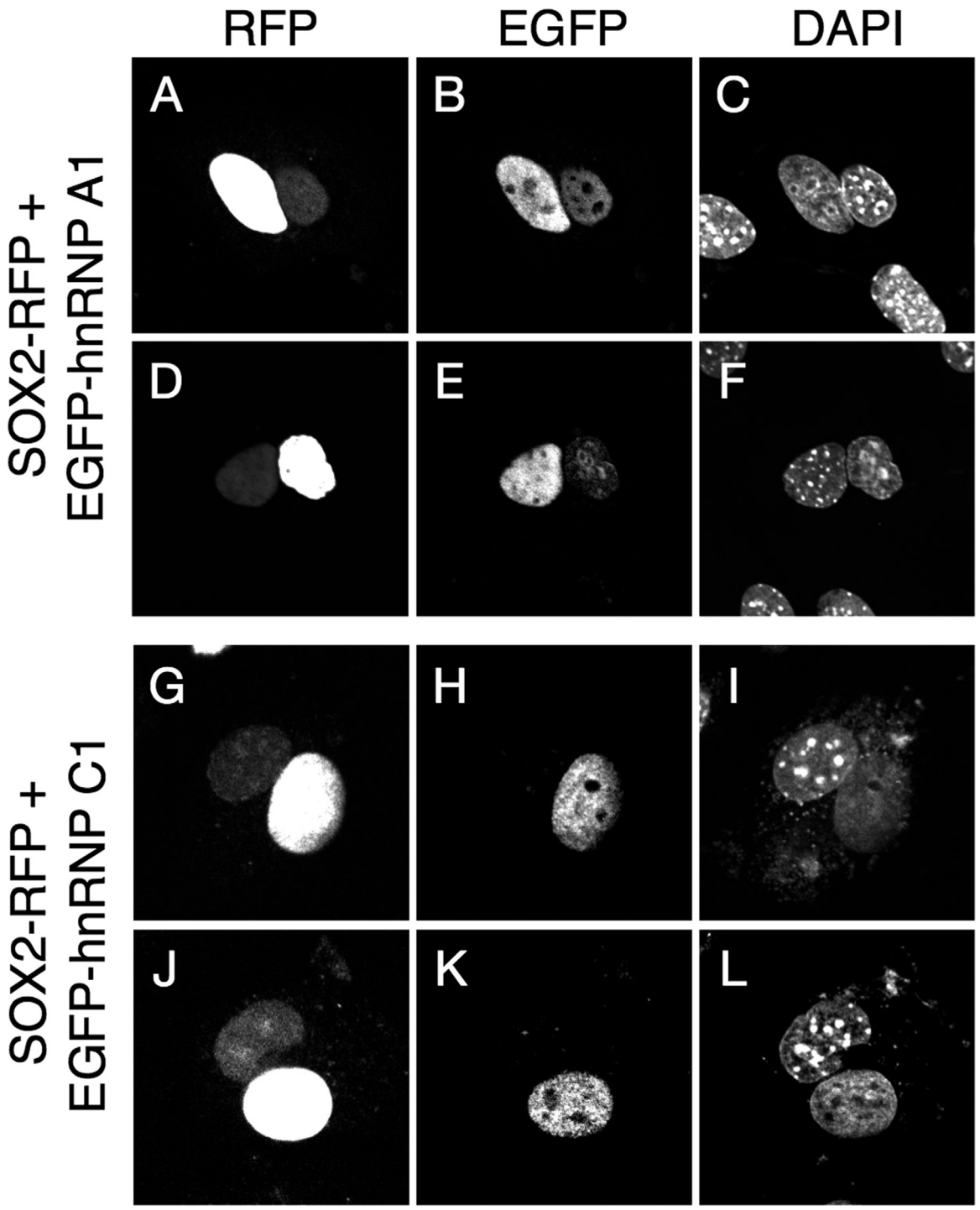

Fig. 4. SOX2 shuttles between the nucleus and the cytoplasm. EGFP-hnRNP A1 or EGFP-hnRNP C1 was transiently co-expressed with SOX2-RFP in HeLa cells for 48 h. NIH3T3 cells were then seeded with the transfected HeLa cells for two hours, followed by cyclohexamide treatment. The culture was then treated with PEG to induce cell fusion. After PEG-induced cell fusion, the culture was incubated for additional 4 h and fixed. The nuclei were stained with Hoechst 33258. The images were acquired using an Olympus laser scanning confocal microscope.

in the S100A14 mRNA. Down-regulation of S100A14 has been associated with poor prognosis in colorectal cancer and oral squamous cell carcinoma [28,32]. Moreover, restoring of S100A14 expression in oral squamous cell carcinoma cell lines significantly decreases their invasive potential and cell growth [33], suggesting that S100A14 can function as an oncosuppressor. To examine whether S100A14 plays a similar role in urothelial carcinoma, we suppressed S100A14 expression in BFTC905 by expression of an anti-S100A14 shRNA (Fig. 6A). The cell cycle analysis of the BFTC895/shS100A14 cells showed that there was a clear decrease in the number of cells in G1 phase and a simultaneous increase in the number of the cells in S phase (Fig. 6B), indicating a shorter G1 phase. In addition to an increase of cell cycle progression, the BFTC905/shS100A14 cells also exhibited increased mobility in the wound healing assay (Fig. 6C). Taken our data together, our experimental results indicated that SOX2 suppresses cell growth and mobility by promoting the expression of S100A14 through post-transcriptional regulation.

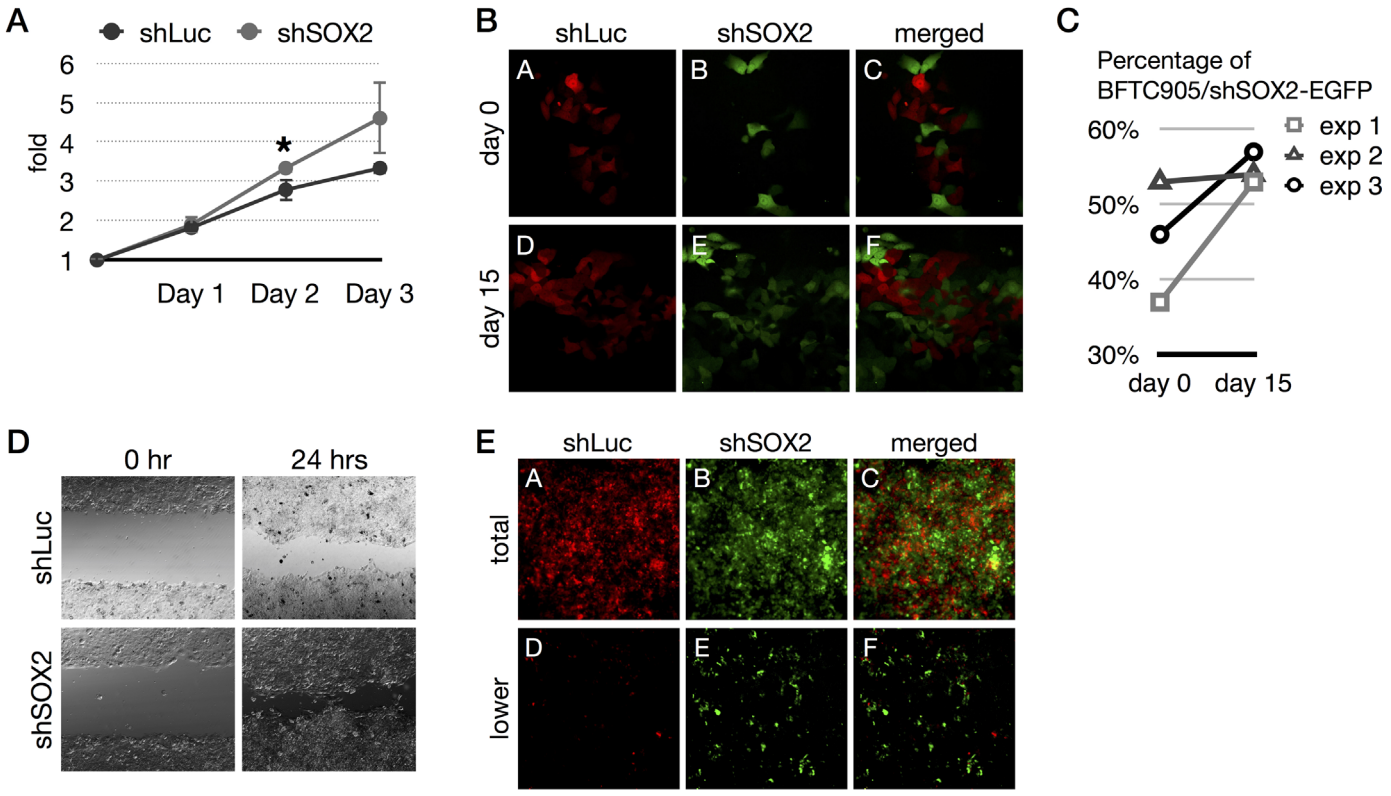

Fig. 5. Suppression of SOX2 leads to an increase in the growth and mobility of BFTC905 cells. (A) The day after seeding the BFTC905/shLuc and BFTC905/shSOX2 cells was designated as day 0. The cell density of an initial 1 × 106 cells was determined by crystal violet staining. The cultures with 5×10^5, 2.5×10^5, or 1.25 × 105 cells were allowed to grow for additional one, two, and three days, respectively. At each time point, the cell densities were determined by crystal violet staining, and the readings were normalized by multiplying the value with the number of respective days. The relative increase in the cell density was calculated by dividing the normalized crystal violet reading with the reading of the day 0 culture. Student's *t*-test was carried out to determine the statistical significance of the differential growth at each point. The *p* value smaller than 0.05 is represented as an asterisk. (B) The BFTC905/shLuc-RFP and BFTC905/shSOX2-EGFP cells were created by transfecting the BFTC905/shLuc and BFTC905/shSOX2 cells with pTag-RFP-N and pEGFP-C1, respectively. After two weeks of antibiotic selection, the cells expressing the fluorescent proteins were collected using a BD FACS Aria III cell sorter. The BFTC905/shLuc-RFP and BFTC905/shSOX2-EGFP cells were then mixed together and cultured in a glass-bottom dish under normal growth and passage conditions for 15 days. At days 0 and 15, the cells were imaged using an Olympus laser scanning confocal microscope. (C) The percentage of BFTC905/shSOX2-EGFP cells in the population was determined by counting more than 200 cells from 10 random images. The results of three independent experiments are shown. (D) The BFTC905/shLuc and BFTC905/shSOX2 cells were seeded in the cell inserts for 24 h. After the inserts were removed, the cells were cultured in medium containing 1% fetal bovine serum for 24 h. The images were captured with a differential interference contrast-equipped microscope at 0 and 24 h. (E) Equal numbers of BFTC905/shLuc-RFP and BFTC905/shSOX2-EGFP cells were seeded into the upper chamber of the transwell apparatus. After attachment, the cells were allowed to migrate in the absence of serum for 24 h. The total cells were first imaged using a fluorescence microscope (panels A–C). After removing the non-migrating cells on the upper side of the transwell membrane, the remaining cells on the lower side were imaged using an Olympus laser scanning confocal microscope (panels D– F).

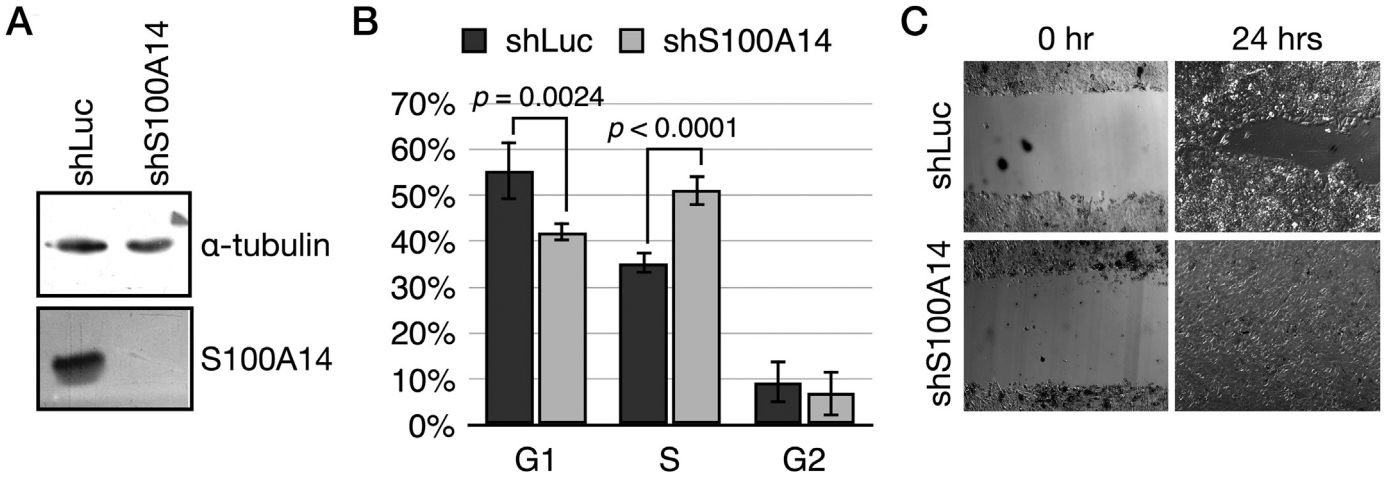

Fig. 6. S100A14 depletion promotes the entry into S phase and accelerates the movement of BFTC905 cells. (A) A lentiviral vector expressing the anti-S100A14 shRNA was delivered into BFTC905 cells to establish the BFTC905/shS100A14 cells. The suppression of S100A14 expression in the BFTC905/shS100A14 cells was determined by immunoblotting. (B) The percentages of BFTC905/shLuc and BFTC905/shS100A14 cells in G1, S, and G2/M phases of the cell cycle was determined by flow cytometry analysis. The statistical difference was determined using the Student's *t*-test. (C) BFTC905/shLuc and BFTC905/shS100A14 cells were seeded in the cell inserts for 24 h. After the inserts were removed, the cells were cultured in medium containing 1% fetal bovine serum for 24 h. The images were captured with a differential interference contrast-equipped microscope at 0, 10, and 24 h.

4. Discussion

In this study, we show that SOX2 binds to the 3′-UTR of the S100A14 mRNA and promotes its expression. Although SOX2 is undoubtedly a transcription factor, our experimental evidence indicates that, in addition to DNA binding, SOX2 also functions as an RNA binding protein. It has been demonstrated that the members of the HMG protein family, including SRY, SOX6, and SOX9, play a role in splicing, thus suggesting that these HMG domain proteins bind to RNA. Our study adds SOX2 to the list of RNA-binding HMG proteins and implies that other HMG proteins function in post-transcriptional regulation as well. It was reported that p53 participates in microRNA biogenesis and that WT1 functions in splicing. Together, these findings raise the possibility that a subset of transcription factors also bind to RNA and participate in post-transcriptional regulation. Post-transcriptional regulation includes alternative splicing, the modulation of mRNA stability, and the control of translation efficiency [31]. Due to the methodology employed in this study, only those genes with their mRNA stability regulated by SOX2 were identified, and we did not rule out that SOX2 may also participate in other post-transcriptional regulation mechanisms.

Previous studies have determined the consensus DNA binding sequence of SOX2 as ACAAAG [34]. However, characterization of the SOX2-occupied chromosome sites in embryonic stem cells, neuronal progenitor cells, and cancer cell lines indicated that SOX2 is targeted to distinct genomic locations in different types of cells [24,35–39]. This is because the targeting specificity of SOX2 is not only determined by its binding preference, but is also dictated by its cofactors. Our result indicates that SOX2 is capable of binding to specific RNA sequences, and the most prominent feature of the SOX2 binding sequence on the S100A14 3′-UTR is a stem-loop structure. This finding suggests that SOX2 acts as a double-stranded RNA binding protein. On the other hand, sequence analysis prediction indicated that multiple RNA protein binding sequences are located in the immediate downstream sequence of the stem-loop structure. Some of these putative RNA binding proteins, including hnRNP A1, hnRNP F, LIN28A, SRSF1, and TRA2A, are highly expressed in BFTC905 cells. A potential seed sequence for hsa-miR-4267 was also predicted in this region. Although which RNA protein binds to this region remained to be determined, it is likely that SOX2 interacts with additional RNA binding protein in the nearby vicinity to form a functional protein complex. How this SOX2-containing RNA binding complex increases the level of the S100A14 mRNA requires further investigation, but the investigation will illustrate the molecular mechanisms of how SOX2 functions in post-transcriptional regulation.

It has been shown that stem cell markers, such as SOX2, are activated more frequently in poorly differentiated tumors and are generally correlated with a poor prognosis [40], suggesting that a reversal to a stem cell property facilitates the growth and invasiveness of tumours. Consistent with this view, the induced expression of SOX2 in the lungs of adult mice was sufficient to drive the development of adenocarcinoma [41]. However, SOX2 expression is required to maintain normal gastric epithelial stem cells, and the loss of SOX2 leads to a complete conversion from gastric to intestinal epithelial characteristics. [42,43]. Epigenetic silencing of SOX2 was frequently observed in intestinal-type gastric cancer, and poor prognosis was associated with the down-regulation of SOX2 [42,44]. Hence, the role of SOX2 in oncogenesis apparently depends on the nature of the cell origin. Expression of SOX2 have been confirmed in urothelial carcinoma, and expression of SOX2 in non-muscle-invasive bladder cancer was correlated with tumor size and poorer survival [45]. Given the heterogeneous nature of cancer, SOX2 expression likely represents a signature of one oncogenic pathway. The observation is consisted with the view that cancer with stem cell property is more aggressive and results in poor outcome. However, a more recent study showed that microRNA-145 increases the expression of the stem cell markers, including SOX2, and induces differentiation of urothelial carcinoma cell line [46]. Thus, whether SOX2 expression is necessarily the signature of the stem cell property in urothelial carcinoma remained to be clarified. It is possible that the cellular function activated by SOX2 in urothelial carcinoma also depends on the context of the cofactor profile.

Among the urothelial carcinoma cell lines we have examined, BFTC905 is the only cell line in which SOX2 was readily detected by both immunoblotting and immunostaining. Morphologically, BFTC905 displays an epithelial morphology and tends to adhere to neighboring cells to form large cell islets. On the other hand, TSGH8301, an urothelial carcinoma cell line from a poor-differentiated stage-II patient, displays weaker attachment to the culture surface nor adheres to the neighboring cells. Since SOX2 promotes the differentiation of the urothelial epithelium [46], SOX2 likely plays a similar function as in gastric epithelium, which is to maintain the normal function of the epithelium. Consequently, loss of SOX2 leads to dysregulation of epithelial cells. In addition to the urothelial carcinoma, loss of SOX2 may also play a role in oncogenesis of other epithelial tissues in which SOX2 is required for normal function and maintenance. Additional studies on other types of carcinoma are needed to collaborate with this compelling hypothesis.

Acknowledgments

This work was supported by the Ministry of Science and Technology, R.O.C. (NSC-101-2311-B-194-001 and NSC-102-2311-B-194-001) and Buddhist Dalin Tzu Chi General Hospital (DTCRD102(2)-I-11 and DTCRD103(3)-E-19).

Transparency document. Supplementary material

Transparency document associated with this article can be found in the online version at http://dx.doi.org/10.1016/j.bbrep.2016.06.016.

Appendix A. Supporting information

Supplementary data associated with this article can be found in the online version at http://dx.doi.org/10.1016/j.bbrep.2016.06.016.

References

[1] J.D. Keene, RNA regulons: coordination of post-transcriptional events, Nat. Rev. Genet. 8 (2007) 533–543.
[2] X.D. Fu, M. Ares Jr., Context-dependent control of alternative splicing by RNA-binding proteins, Nat. Rev. Genet. 15 (2014) 689–701.
[3] A. van den Berg, J. Mols, J. Han, RISC-target interaction: cleavage and translational suppression, Biochim. Biophys. Acta 2008 (1779) 668–677.
[4] W.H. Hudson, E.A. Ortlund, The structure, function and evolution of proteins that bind DNA and RNA, Nat. Rev. Mol. Cell Biol. 15 (2014) 749–760.
[5] A.G. Baltz, M. Munschauer, B. Schwanhausser, A. Vasile, Y. Murakawa, M. Schueler, N. Youngs, D. Penfold-Brown, K. Drew, M. Milek, E. Wyler, R. Bonneau, M. Selbach, C. Dieterich, M. Landthaler, The mRNA-bound proteome and its global occupancy profile on protein-coding transcripts, Mol. Cell 46 (2012) 674–690.
[6] A. Castello, B. Fischer, K. Eichelbaum, R. Horos, B.M. Beckmann, C. Strein, N. E. Davey, D.T. Humphreys, T. Preiss, L.M. Steinmetz, J. Krijgsveld, M.W. Hentze, Insights into RNA biology from an atlas of mammalian mRNA-binding proteins, Cell 149 (2012) 1393–1406.
[7] D. Ray, H. Kazan, K.B. Cook, M.T. Weirauch, H.S. Najafabadi, X. Li, S. Gueroussov, M. Albu, H. Zheng, A. Yang, H. Na, M. Irimia, L.H. Matzat, R. K. Dale, S.A. Smith, C.A. Yarosh, S.M. Kelly, B. Nabet, D. Mecenas, W. Li, R.

S. Laishram, M. Qiao, H.D. Lipshitz, F. Piano, A.H. Corbett, R.P. Carstens, B.J. Frey, R.A. Anderson, K.W. Lynch, L.O. Penalva, E.P. Lei, A.G. Fraser, B.J. Blencowe, Q. D. Morris, T.R. Hughes, A compendium of RNA-binding motifs for decoding gene regulation, Nature 499 (2013) 172–177.
[8] C. Maris, C. Dominguez, F.H. Allain, The RNA recognition motif, a plastic RNA-binding platform to regulate post-transcriptional gene expression, FEBS J. 272 (2005) 2118–2131.
[9] G.M. Daubner, A. Clery, F.H. Allain, RRM-RNA recognition: NMR or crystallography…and new findings, Curr. Opin. Struct. Biol. 23 (2013) 100–108.
[10] G. Nicastro, I.A. Taylor, A. Ramos, KH-RNA interactions: back in the groove, Curr. Opin. Struct. Biol. 30 (2015) 63–70.
[11] T.M. Hall, Multiple modes of RNA recognition by zinc finger proteins, Curr. Opin. Struct. Biol. 15 (2005) 367–373.
[12] J. Font, J.P. Mackay, Beyond DNA: zinc finger domains as RNA-binding modules, Methods Mol. Biol. 649 (2010) 479–491.
[13] Y. Miyamoto, H. Taniguchi, F. Hamel, D.W. Silversides, R.S. Viger, A GATA4/WT1 cooperation regulates transcription of genes required for mammalian sex determination and differentiation, BMC Mol. Biol. 9 (2008) 44.
[14] Y.Y. Chau, N.D. Hastie, The role of Wt1 in regulating mesenchyme in cancer, development, and tissue homeostasis, Trends Genet 28 (2012) 515–524.
[15] F.J. Motamedi, D.A. Badro, M. Clarkson, M.R. Lecca, S.T. Bradford, F.A. Buske, K. Saar, N. Hubner, A.W. Brandli, A. Schedl, WT1 controls antagonistic FGF and BMP-pSMAD pathways in early renal progenitors, Nat. Commun. 5 (2014) 4444.
[16] R.C. Davies, C. Calvio, E. Bratt, S.H. Larsson, A.I. Lamond, N.D. Hastie, WT1 interacts with the splicing factor U2AF65 in an isoform-dependent manner and can be incorporated into spliceosomes, Genes Dev. 12 (1998) 3217–3225.
[17] M.A. Markus, B. Heinrich, O. Raitskin, D.J. Adams, H. Mangs, C. Goy, M. Ladomery, R. Sperling, S. Stamm, B.J. Morris, WT1 interacts with the splicing protein RBM4 and regulates its ability to modulate alternative splicing in vivo, Exp. Cell Res. 312 (2006) 3379–3388.
[18] A.A. Morrison, R.L. Viney, M.R. Ladomery, The post-transcriptional roles of WT1, a multifunctional zinc-finger protein, Biochim. Biophys. Acta 2008 (1785) 55–62.
[19] H.I. Suzuki, K. Yamagata, K. Sugimoto, T. Iwamoto, S. Kato, K. Miyazono, Modulation of microRNA processing by p53, Nature 460 (2009) 529–533.
[20] M. Stros, D. Launholt, K.D. Grasser, The HMG-box: a versatile protein domain occurring in a wide variety of DNA-binding proteins, Cell Mol. Life Sci. 64 (2007) 2590–2606.
[21] M. Wegner, All purpose Sox: the many roles of Sox proteins in gene expression, Int. J. Biochem. Cell Biol. 42 (2010) 381–390.
[22] K. Ohe, E. Lalli, P. Sassone-Corsi, A direct role of SRY and SOX proteins in pre-mRNA splicing, Proc. Natl. Acad. Sci. USA 99 (2002) 1146–1151.
[23] S. Veretnik, M. Gribskov, RNA binding domain of HDV antigen is homologous to the HMG box of SRY, Arch. Virol. 144 (1999) 1139–1158.
[24] L.A. Boyer, T.I. Lee, M.F. Cole, S.E. Johnstone, S.S. Levine, J.P. Zucker, M. G. Guenther, R.M. Kumar, H.L. Murray, R.G. Jenner, D.K. Gifford, D.A. Melton, R. Jaenisch, R.A. Young, Core transcriptional regulatory circuitry in human embryonic stem cells, Cell 122 (2005) 947–956.
[25] N. Tapia, C. MacCarthy, D. Esch, A. Gabriele Marthaler, U. Tiemann, M. J. Arauzo-Bravo, R. Jauch, V. Cojocaru, H.R. Scholer, Dissecting the role of distinct OCT4-SOX2 heterodimer configurations in pluripotency, Sci. Rep. 5 (2015) 13533.
[26] C.L. Tung, P.H. Hou, Y.L. Kao, Y.W. Huang, C.C. Shen, Y.H. Cheng, S.F. Wu, M. S. Lee, C. Li, SOX2 modulates alternative splicing in transitional cell carcinoma, Biochem. Biophys. Res. Commun. 393 (2010) 420–425.
[27] E. McKiernan, E.W. McDermott, D. Evoy, J. Crown, M.J. Duffy, The role of S100 genes in breast cancer progression, Tumour Biol. 32 (2011) 441–450.
[28] D. Sapkota, O. Bruland, D.E. Costea, H. Haugen, E.N. Vasstrand, S.O. Ibrahim, S100A14 regulates the invasive potential of oral squamous cell carcinoma derived cell-lines in vitro by modulating expression of matrix metalloproteinases, MMP1 and MMP9, Eur. J. Cancer 47 (2011) 600–610.
[29] A. Chaudhury, G.S. Hussey, P.H. Howe, 3′-UTR-mediated post-transcriptional regulation of cancer metastasis: beginning at the end, RNA Biol. 8 (2011) 595–599.
[30] E. Matoulkova, E. Michalova, B. Vojtesek, R. Hrstka, The role of the 3′ untranslated region in post-transcriptional regulation of protein expression in mammalian cells, RNA Biol. 9 (2012) 563–576.
[31] S.F. Mitchell, R. Parker, Principles and properties of eukaryotic mRNPs, Mol. Cell 54 (2014) 547–558.
[32] H.Y. Wang, J.Y. Zhang, J.T. Cui, X.H. Tan, W.M. Li, J. Gu, Y.Y. Lu, Expression status of S100A14 and S100A4 correlates with metastatic potential and clinical outcome in colorectal cancer after surgery, Oncol. Rep. 23 (2010) 45–52.
[33] D. Sapkota, D.E. Costea, M. Blo, O. Bruland, J.B. Lorens, E.N. Vasstrand, S. O. Ibrahim, S100A14 inhibits proliferation of oral carcinoma derived cells through G1-arrest, Oral. Oncol. 48 (2012) 219–225.
[34] M. Salmon-Divon, H. Dvinge, K. Tammoja, P. Bertone, PeakAnalyzer: genome-wide annotation of chromatin binding and modification loci, BMC Bioinform. 11 (2010) 415.
[35] Y. Kamachi, M. Uchikawa, A. Tanouchi, R. Sekido, H. Kondoh, Pax6 and SOX2 form a co-DNA-binding partner complex that regulates initiation of lens development, Genes Dev. 15 (2001) 1272–1286.
[36] X. Fang, J.G. Yoon, L. Li, W. Yu, J. Shao, D. Hua, S. Zheng, L. Hood, D.R. Goodlett, G. Foltz, B. Lin, The SOX2 response program in glioblastoma multiforme: an integrated ChIP-seq, expression microarray, and microRNA analysis, BMC Genom. 12 (2011) 11.
[37] I. Aksoy, R. Jauch, J. Chen, M. Dyla, U. Divakar, G.K. Bogu, R. Teo, C.K. Leng Ng, W. Herath, S. Lili, A.P. Hutchins, P. Robson, P.R. Kolatkar, L.W. Stanton, Oct4 switches partnering from Sox2 to Sox17 to reinterpret the enhancer code and specify endoderm, EMBO J. 32 (2013) 938–953.
[38] M.A. Lodato, C.W. Ng, J.A. Wamstad, A.W. Cheng, K.K. Thai, E. Fraenkel, R. Jaenisch, L.A. Boyer, SOX2 co-occupies distal enhancer elements with distinct POU factors in ESCs and NPCs to specify cell state, PLoS Genet. 9 (2013) e1003288.
[39] K. Jung, P. Wang, N. Gupta, K. Gopal, F. Wu, X. Ye, A. Alshareef, G. Bigras, T. P. McMullen, B.S. Abdulkarim, R. Lai, Profiling gene promoter occupancy of Sox2 in two phenotypically distinct breast cancer cell subsets using chromatin immunoprecipitation and genome-wide promoter microarrays, Breast Cancer Res. 16 (2014) 470.
[40] K. Almstrup, C.E. Hoei-Hansen, U. Wirkner, J. Blake, C. Schwager, W. Ansorge, J. E. Nielsen, N.E. Skakkebaek, E. Rajpert-De Meyts, H. Leffers, Embryonic stem cell-like features of testicular carcinoma in situ revealed by genome-wide gene expression profiling, Cancer Res. 64 (2004) 4736–4743.
[41] Y. Lu, C. Futtner, J.R. Rock, X. Xu, W. Whitworth, B.L. Hogan, M.W. Onaitis, Evidence that SOX2 overexpression is oncogenic in the lung, PLoS One 5 (2010) e11022.
[42] T. Otsubo, Y. Akiyama, K. Yanagihara, Y. Yuasa, SOX2 is frequently down-regulated in gastric cancers and inhibits cell growth through cell-cycle arrest and apoptosis, Br. J. Cancer 98 (2008) 824–831.
[43] S. Asonuma, A. Imatani, N. Asano, T. Oikawa, H. Konishi, K. Iijima, T. Koike, S. Ohara, T. Shimosegawa, Helicobacter pylori induces gastric mucosal intestinal metaplasia through the inhibition of interleukin-4-mediated HMG box protein Sox2 expression, Am. J. Physiol. Gastrointest. Liver Physiol. 297 (2009) G312–G322.
[44] S. Wang, J. Tie, R. Wang, F. Hu, L. Gao, W. Wang, L. Wang, Z. Li, S. Hu, S. Tang, M. Li, X. Wang, Y. Nie, K. Wu, D. Fan, SOX2, a predictor of survival in gastric cancer, inhibits cell proliferation and metastasis by regulating PTEN, Cancer Lett. 358 (2015) 210–219.
[45] J. Ruan, B. Wei, Z. Xu, S. Yang, Y. Zhou, M. Yu, J. Liang, K. Jin, X. Huang, H. Cheng, Predictive value of Sox2 expression in transurethral resction specimens in patients with T1 bladder cancer, Med. Oncol. 30 (2013) 445.
[46] T. Fujii, K. Shimada, Y. Tatsumi, K. Hatakeyama, C. Obayashi, K. Fujimoto, N. Konishi, microRNA-145 promotes differentiation in human urothelial carcinoma through down-regulation of syndecan-1, BMC Cancer 15 (2015) 818.